High Energy Hadron Colliders

1 Introduction

- Full exploitation of LHC program:

- Strong LARP program, support of HL-LHC construction project in US + continuation of LARP towards 20T magnets for HE-LHC or new collider in big tunnel, needs to be HEP priority;

- participate in CERN-led international study on 100 TeV pp collider in big tunnel (opens up option for e^+e^- storage ring, if no ILC);

- US R&D portfolio for hadrons / long-term roadmap;

- Identify R&D overlaps with leptons and intensity frontier, MuC need of high field magnets (dipoles and solenoid + FF quads).

The dipole magnets are the dominant cost drivers for future Hadron colliders. The developments that have occurred in high-field dipole magnet performance in the US over the last two decades, as shown in Fig. 1, have been made possible by the strong support of DOE HEP through the GARD program. The dipole field strengths obtained through these programs enables the community to consider collider configurations with energies significantly beyond the LHC, as shown in Fig. 8. We note that the infrastructure and expertise needed to make significant progress in this field are the result of long-term vision and support from HEP funding agencies. Based on the developments to date, one can make some general statements of the current status and potential future of magnet development:

- The technology basis is in place for dipole magnets generating $\sim 15T$ fields (with operating margin). To bring the technology to a state of readiness for application in a future collider will require a focussed technology readiness effort similar to that of LARP, and of a similar timescale (~ 10 years) and funding level.

- The technology basis for 20+ T dipoles is not yet in place, although excellent concepts are being proposed that warrant investigation. Strong R&D support for these efforts, similar to that provided to the magnet research groups over the last decade, can be expected to yield results within a ~ 5 year timeframe. If the development is successful, one should anticipate again a follow-on phase of technology readiness in order to bring the technology to a state needed for implementation in a project. For magnets in this field realm conductor developments are critical, and magnet support must be matched with support for conductor R&D.
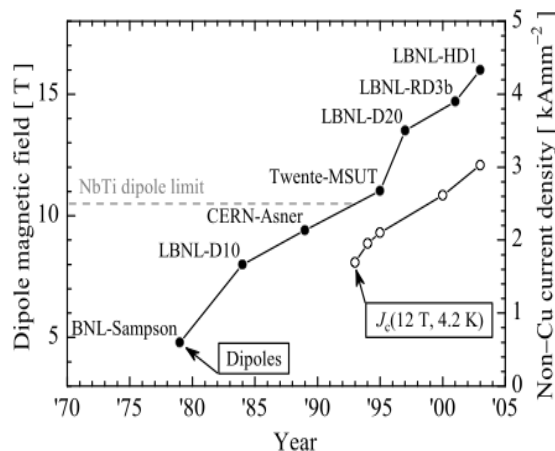
Figure 1: Progress in superconducting dipole magnet performance and in the increase in $J_c(12T, 4.2K)$ of Nb$_3$Sn over the last 20+ years.

The dipole magnet R&D is well-leveraged, in the sense that it serves both Hadron and Muon collider scenarios. Finally, we note that in addition to field strength, magnet programs need to take into consideration cost-effectiveness and scalability in magnet designs. As noted earlier, the superconducting dipoles for a future collider will dominate the facility cost; furthermore, they are technically one of the highest-risk elements. Designs must be industrializable to leverage the strength of the private sector in providing cost-effective fabrication.

2   The physics landscape

The observation of the Higgs boson at the LHC opens a new era for particle physics. Its measured properties are consistent, within the current uncertainties, with those of the Standard Model (SM) Higgs boson. This gives a remarkable confirmation of an apparently naive theoretical setup, formulated over forty years ago, to explain the otherwise inconsistent coexistence of a gauge theory for electroweak (EW) interactions, with the masses of the gauge bosons, of quarks and of charged leptons. On the other hand, the complete lack of evidence for new physics makes more concrete and urgent the understanding of the naturalness of the EW scale, whose smallness with respect to the Planck scale requires, in the context of the SM, an incredible amount of fine tuning. The existence of new physics beyond the SM (BSM) is also needed in view of the SM inadequacy to explain phenomena like dark matter, the matter-antimatter asymmetry and neutrino masses.

After the discovery of the Higgs boson, understanding what is the real origin of EW symmetry breaking (EWSB) becomes the next key challenge for collider physics. This challenge can be expressed in terms of two questions: up to which level of precision does the Higgs boson behave like predicted by the SM? Where are the new particles that should solve the EW naturalness problem and, possibly, offer some insight in the origin of dark matter, the

matter-antimatter asymmetry, and neutrino masses? The first question allows us to define concrete deliverables for the LHC and future colliders. We know there is a Higgs boson at about 125 GeV and we can thus analyze in great detail the prospects for more precise measurements of all of its properties at the various facilities. The second question does not come with the guarantee of concrete discovery deliverables, but its relevance is powerful enough to justify pursuing the search efforts as ambitiously as possible.

The approved LHC programme, its future upgrade towards higher luminosities, and the study for a new hadron collider delivering collisions at significantly higher energy, are all essential components of this endeavour. High-luminosity offers the potential to increase the precision of several key measurements, to uncover rare processes, and to guide and validate the progress in theoretical modeling, thus reducing the systematic uncertainties in the interpretation of the data. The extended lever arm afforded by an higher beam energy, increases the potential to directly probe greater and greater mass scales for BSM processes, and gives access to the TeV energy scale, which is the natural domain to test the dynamics of EWSB (e.g. high-mass $WW \to WW$ and $WW \to HH$ scattering, triple and quartic gauge and Higgs couplings). Detailed studies of the realistic performance in the measurements of Higgs couplings, self-coupling and WW scattering at energies above 14 TeV do not yet exist and will be required to precisely assess their accuracy and potential. More in general, higher statistics, whether coming from higher luminosity or from increased cross sections at higher energies, open new opportunities for both searches and measurements, enabling analysis strategies where tighter cuts can greatly improve the signal purity and/or reduce the theoretical uncertainties. The long history of the Tevatron gives clear evidence of the immense progress that can be made, relative to naive earlier estimates, after the accumulation of bigger amounts of data and of more experience with their analysis.

The lack of a guarantee that *any* future facility will directly observe new particles, greatly strengthens the relevance of a broad programme of very precise measurements. The exploration of the Higgs sector provides us with a benchmark for the assessment of the physics potential of future facilities, including hadron colliders at the energy frontier. Several directions should be pursued, including the high-precision study of the couplings already observed, the search of rare (e.g. $H \to \mu^+\mu^-$) or forbidden Higgs decays and the study of the dynamics of Higgs interactions (including Higgs-pair production processes, sensitive to the Higgs self-coupling and to other possible anomalous interactions).

What really defines the Higgs boson is its role in the breaking of the EW symmetry. In particular, its coupling to the longitudinal polarization of W and Z bosons and the resulting unitarization of high-energy WW scattering. This is a key element in the study of EWSB. The theoretical description of WW scattering requires the exchange of the Higgs boson, or of some other new particle, in order to tame the otherwise unphysical rate growth at energies around the TeV and above. Verifying the details of this process is essential to learn more on whether the Higgs boson is indeed a fundamental particle or, as postulated in some theories, a composite object, something that could also manifest itself with the appearance of new resonances in the TeV range. As has been known and documented for many years, these studies require the highest possible energies. For example, in a class of composite-

Process	σ(14 TeV)	R(33)	R(40)	R(60)	R(80)	R(100)
$gg \rightarrow H$	50.4 pb	3.5	4.6	7.8	11	15
$qq \rightarrow qqH$	4.40 pb	3.8	5.2	9.3	14	19
$q\bar{q} \rightarrow WH$	1.63 pb	2.9	3.6	5.7	7.7	10
$q\bar{q} \rightarrow ZH$	0.90 pb	3.3	4.2	6.8	10	13
$pp \rightarrow HH$	33.8 fb	6.1	8.8	18	29	42
$pp \rightarrow ttH$	0.62 pb	7.3	11	24	41	61

Table 1: Evolution with beam energy of the cross sections for different Higgs production processes in pp collisions. We list cross sections at $\sqrt{S} = 14$ TeV in the second column, and the ratios $R(E) = \sigma(E \text{ TeV})/\sigma(E = 14 \text{ TeV})$ in the following columns. All rates assume $m_H = 125$ GeV and SM couplings.

Higgs models, deviations from the SM behaviour of the WW scattering cross section, due to anomalous Higgs interactions, scale like $\xi^2(E_{CM}(WW)/600 \text{ GeV})^4$. ξ is related to the scale of new physics[1], and determines also a change of order ξ, w.r.t. the SM, in B($H \rightarrow WW^*$). It takes centre-of-mass energies of the WW system well above 1 TeV to have sensitivity to these deviations. At 14 TeV and 300 fb^{-1}, the statistics of events with $E_{CM}(WW) > 1$ TeV is limited and experiments will be sensitive to values of $\xi \gtrsim 0.5$. This sensitivity improves to $\mathcal{O}(0.10)$ and $\mathcal{O}(0.01)$, for pp collisions at 30 and 100 TeV, respectively. The design energy of the SSC, 40 TeV, was chosen to optimize the reach and precision of these measurements. The need to perform these EWSB studies today is even stronger than it was in the days of the SSC planning, due to the observation of a light Higgs particle. No realistic assessment of the potential of possible future experiments for these measurements is currently available. The issues to be considered include the geometrical acceptance of forward/backward jets and the ability to reconstruct them in presence of large pileup.

Table 2 [1] summarizes the increase in rate for several Higgs production channels in pp collisions, as a function of the beam energy, covering the range of possibilities being considered in this document. Final states with the largest invariant mass (like ttH and HH) benefit the most from the energy increase. This benefit is further enhanced when we consider the fraction of events passing the typical analysis cuts imposed to improve signal separation or to reduce systematic uncertainties. For example, in the case of ttH production, requiring the top quarks to have a transverse momentum above 500 GeV would increase the rates by a factor of 16 (250) at 33 TeV (100 TeV), instead of the factor of 7 (60) increase for the fully inclusive ttH rate.

In many BSM scenarios for EWSB, the Higgs boson is accompanied by several new particles, with masses in the range of hundred(s) GeV to possibly several TeV. These could be other Higgs-like scalar states, or heavier partners of the W and Z gauge bosons and of the top and bottom quarks, or, as in the case of supersymmetry, a complete replica of the SM particle spectrum, where each known particle has a partner, with a different spin quantum number. Any deviation of the measured Higgs properties from the SM expectation would

---
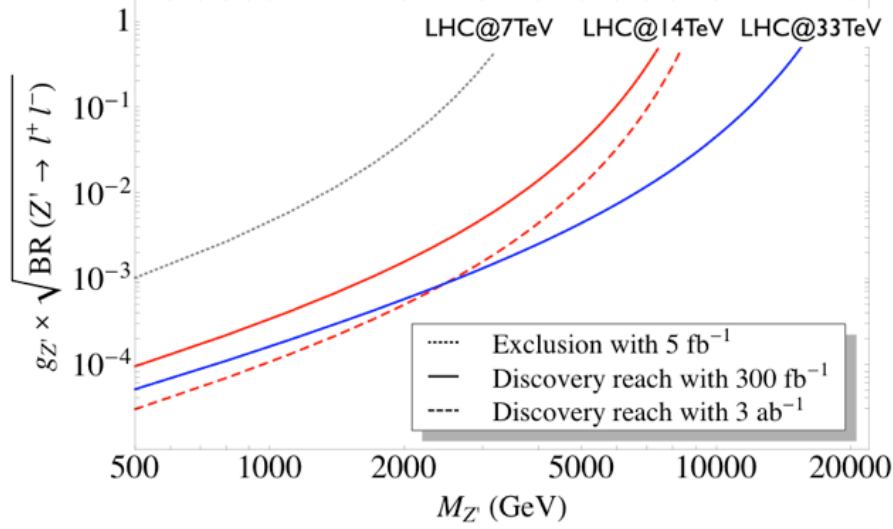[1]$\xi = v^2/f^2$, where $v = 246$ GeV is the EWSB scale, and f is the compositeness scale.

Figure 2:
Discovery potential for new Z' gauge bosons decaying to lepton pairs, as a function of their mass. The reach is expressed in terms of their coupling strength times the leptonic branching ratio.

imply the existence of at least some of these particles, and viceversa. The mass limits on such new particles derived so far from the LHC still leave ample room for their discovery in the 14 TeV data. However, any discovery at 14 TeV will require a follow-up phase of precision measurements, to understand the origin of the newly observed phenomena. For example, while new Z' gauge bosons, signalling the existence of new weak interactions, can be discovered with 300 fb^{-1} up to 4-5 TeV, the full HL-LHC luminosity will be needed to determine their properties if their mass is above 2.5 TeV. Existing studies also show that a tenfold increase in the LHC integrated luminosity will extend by 30-50% the discovery reach for new particles.

In the study of the energy frontier with hadron collisions energy and luminosity play a complementary role. Production rates for the signals of interest at the collider may be small either because the mass of the produced objects is large or because the coupling strength is small. In the former case, an increase in the beam energy is clearly favourable, while to probe small couplings at smaller masses higher luminosity may be more effective. For a signal at a fixed mass scale M, the cross section $\sigma(M, g) \propto g^2/M^2 \times L(x = M/\sqrt{S})$ grows with the hadronic center of mass energy $\sqrt{S}$, since the *partonic* luminosity $L(x)$ grows at least like $\log(1/x)$. An increase in accelerator energy does not need, in this case, to be accompanied by an increase in luminosity. On the other hand, to scale the discovery mass reach M with the beam energy means keeping $x = M/\sqrt{S}$ fixed. In this case the cross section scales like $\sigma(M, g) \propto g^2/S \times L(x)/x \propto 1/S$ and the collider luminosity must grow as the square of the energy.

Depending on the mass and couplings of these new particles the most effective way to increase their statistics could either be higher luminosity, or higher energy. This is illustrated in a simple concrete case in Fig.2, which represents the LHC discovery potential for Z' gauge bosons decaying to lepton pairs, in different energy and integrated luminosity conditions. The reach is expressed by the product of their coupling strength, g, and the square root of the leptonic decay branching ratio. The dashed line corresponds to the results after 3000 fb^{-1} at 14 TeV, the solid blue line to 300 fb^{-1} at 33 TeV. We notice that for masses below ~ 2.5 TeV the factor of 10 higher luminosity at 14 TeV leads to a better discovery reach (or, in the case of a previous discovery, leads to higher statistics and better precision in the measurement of the Z' properties). On the contrary, if the Z' is heavier than ~ 2.5 TeV, the increase is energy is more effective. The figure also shows that the run at 7 TeV has already excluded the existence of Z' bosons up to 2.5 TeV, at least for some range of their couplings. This means that, at least for some models, a new particle discovered at 14 TeV would be sufficiently heavy that its precision studies would greatly benefit from the energy upgrade, even after the completion of an extensive high luminosity LHC phase. Similar reasoning applies to other BSM new particles. A higher energy LHC is therefore a powerful tool to extend and improve the precision studies of the Higgs boson and other phenomena to be uncovered during the nominal and high-luminosity LHC runs at 14 TeV, as well as to open the way for the exploration of a new energy range, unattainable by any of the other current proposals for new high-energy facilities.

The exploration of physics beyond the SM at the high energy frontier will unavoidably require going towards hadron collisions at higher energies. The current limits obtained by LHC at 8 TeV already point in a natural way to high energy upgrades as the best way to perform quantitative studies of possible discoveries made at 14 TeV. Even in the absence of such discoveries, the exploratory potential of a high energy pp collider will provide the only opportunity to shed more light on the origin on EW symmetry breaking and of the hierarchy problem at the energy frontier.

3 Underlying events in high energy collisions

Underlying events (UE) represent a major challenge for experiments at high-luminosity hadron colliders both in terms of occupancy and of precision in the reconstruction of the event kinematics. The beam parameters for the LHC high-luminosity upgrade, discussed below, are chosen to mitigate the number of underlying events and keep them within manageable limits. The evaluation of the rate and characteristics of minimum bias events as a function of the centre-of-mass energy is therefore important for guiding the choice of beam parameters from 14 TeV towards higher energies.

The total cross section of minimum bias events, can be obtained with a simple Donnachie-Landshoff fit with $\epsilon \sim 0.08$ [2], similarly to the scaling ansätze made in PYTHIA [3]. The ALICE measurements of the inelastic and single-diffractive cross sections [4] do not show any significant deviations from this ansatz over the kinematic range of their measurements.
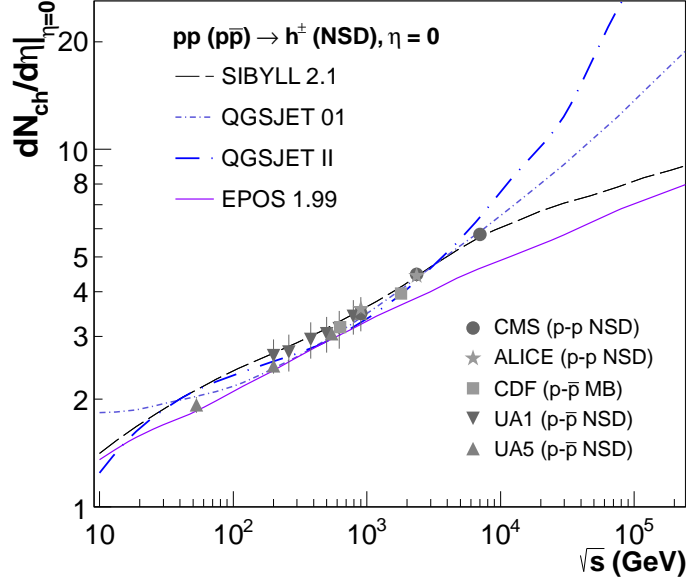
Figure 3: Scaling of the central charged multiplicity for SIBYLL, QGSJET, and EPOS, compared with collider data for NSD events (from [5]).

The extrapolations yield an inelastic cross section growing from $\sim$70 mb at 7 TeV to $\sim$90 mb at 30 TeV and $\sim$105 mb at 100 TeV. The diffractive components increase by only a few mb relative to the LHC values. These collisions can be characterised in terms of their track multiplicity and associated energy deposition. The extrapolations of central charged-track densities in so-called non-single-diffractive events in pomeron-based models are shown in the left-hand panel of fig. 3 (from [5]). Combining the uncertainty variations of various generator tunes yields an estimated central charged-track density per unit $\Delta\eta\Delta\phi$ of 1.32 ± 0.13 at 30 TeV, and 1.8 ± 0.4 at 100 TeV, for inelastic events with at least one track inside the $|\eta| < 1$ acceptance. Moving to different pseudo-rapidity intervals does not significantly change these predictions.

An important quantity for jet energy scale calibrations is the amount of transverse energy deposited in the detector, per unit $\Delta R^2 = \Delta\eta \times \Delta\phi$, per inelastic collision (corresponding to the blue cross-section curve in fig. ??). In the central region of the detector, the Perugia models are in good agreement with the ATLAS measurements at 7 TeV [6, 7], while the activity in the forward region appears to be underestimated [8, 6, 9, 7]. Extrapolations lead to an estimated $1.25 \pm 0.2\,\mathrm{GeV}$ of transverse energy deposited per unit ΔR^2 in the central region of the detector at 30 TeV, growing to $1.9 \pm 0.35\,\mathrm{GeV}$ at 100 TeV, as shown in the middle panel of fig. 4.

The last quantity we consider is the activity in the underlying event. The most important UE observable is the summed $p_\perp$ density in the so-called "TRANSVERSE" region, defined as the wedge $60 - 120°$ away in azimuth from a hard trigger jet. For $p_\perp^{\mathrm{jet}}$ values above 5 – 10 GeV, this distribution is effectively flat, i.e., to first approximation it is independent of the jet $p_\perp$. It does, however, depend significantly on the centre-of-mass energy of the pp
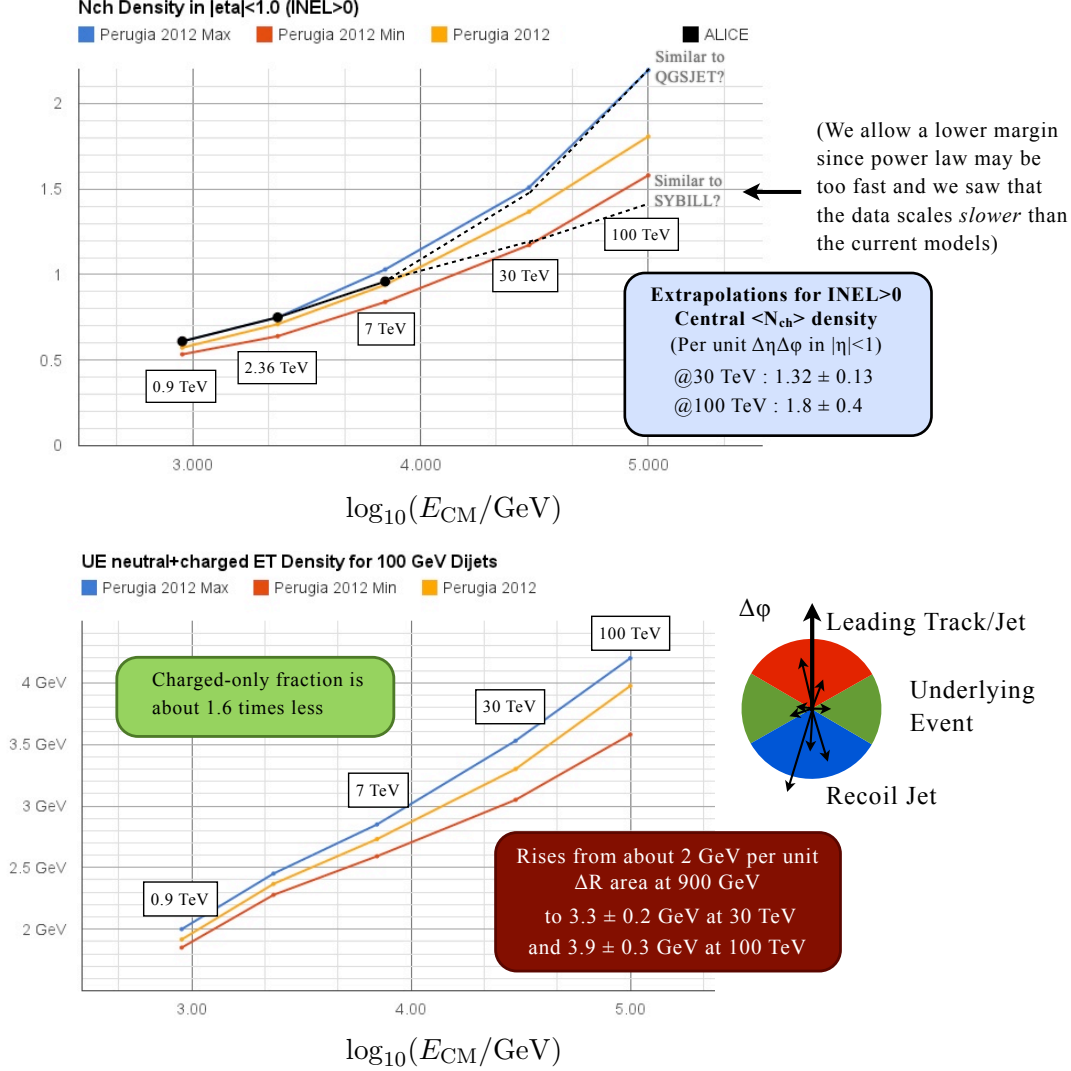
Figure 4: Extrapolations of the central charged-track density for INEL>0 events (*Top*), central E_T density for INEL events (*Middle*), and central UE E_T density for 100-GeV dijet events (*Bottom*).

collision, a feature which places strong constraints on the scaling of the $p_{\perp 0}$ scale of MPI models. Given the good agreement between the Perugia 2012 models and Tevatron and LHC UE measurements [7], we estimate the E_T (neutral+charged) density in the TRANSVERSE region (inside $|\eta| < 2.5$), for a reference case of 100-GeV dijets in the bottom pane of fig. 4: starting from an average of about $2\,\mathrm{GeV}$ per ΔR^2 at 900 GeV, the density rises to $3.3 \pm 0.2\,\mathrm{GeV}$ at 30 TeV and to $3.9 \pm 0.3\,\mathrm{GeV}$ at 100 TeV, while the charged-only fraction should be about a factor 1.6 less.
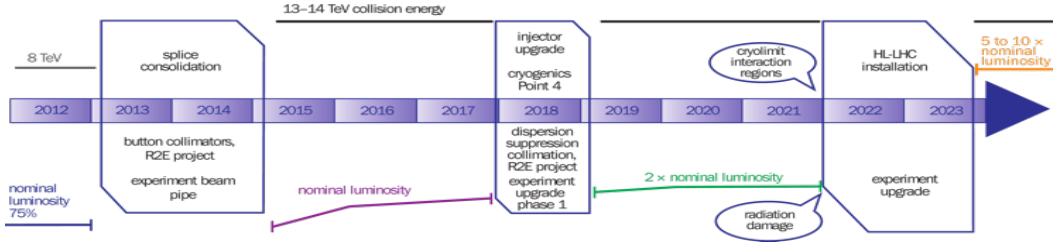
Figure 5: LHC baseline plan for the next ten years. In terms of energy of the collisions (upper line) and of luminosity (lower lines). The first long shutdown (LS) 2013-14 is to allow design parameters of beam energy and luminosity. The second LS, 2018, is to increase beam intensity and reliability as well as to upgrade the LHC Injectors.
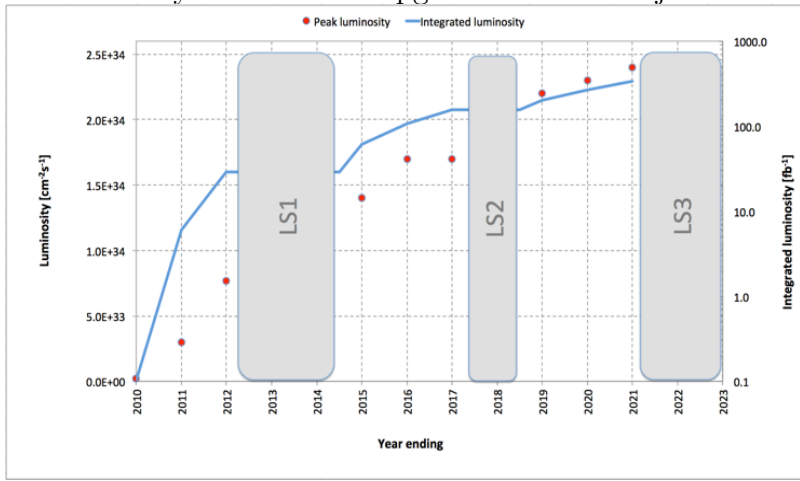

Figure 6: Forecast of peak luminosity evolution and best consequent integrated luminosity.

4 LHC luminosity upgrade

The full exploitation of the LHC is the highest priority of the energy frontier collider program. LHC is expected to restart in Spring 2015 at center-of-mass energy of 13-14 TeV and that it will reach the design luminosity1 of 10^{34} cm^{-2}s^{-1} during 2015. This peak value should give a total integrated luminosity over one year of about 40 fb^{-1}. In the period 2015-2020, the LHC will gradually increase its peak luminosity. Margins have been taken in the design to allow the machine to reach about two times the nominal design performance. The baseline program for the next decade is schematically shown in Figure 5, while in Figure 6 gives the possible evolution of the peak and integrated luminosity.

After 2020 some critical components of the accelerator will reach the radiation damage limit and other will be see their reliability lessening because of vulnerability to radiation, wear and high intensity beam operation. Therefore, important consolidation actions are required before 2020, just to keep the LHC running with a good availability. Further, the statistical gain in running the accelerator without an additional considerable luminosity increase beyond its design value will become marginal, therefore the LHC will need to have a decisive increase of its luminosity.

9

This new phase of the LHC life, named as High Luminosity LHC (HL-LHC) has the scope of preparing the machine to attain the astonishing threshold of 3000 fb-1 during 10-12 years of operation. The project is now the first priority of Europe, as stated by the Strategy update for High Energy Physics group approved by CERN council in the special session of 30 May 2013 in Brussels.

4.1 HL-LHC

The LHC proton nominal design luminosity luminosity for each of the two general purpose experiments (ATLAS and CMS) is $L_0=10^{34}$ cm^{-2}s^{-1}. This luminosity is associated with a bunch spacing of 25 ns (2808 bunches per beam) gives an average value of 271 events/crossing, or pile up. The main objectives of High Luminosity LHC are the following:

1. peak luminosity of 5×10^{34}cm^{-2}s^{-1} with leveling,

2. integrated luminosity of 250 fb^{-1}/year, enabling the goal of 3000 fb^{-1} within twelve years after the upgrade.

This luminosity is about ten times the luminosity reach of the first twelve years of the LHC lifetime. The luminosity upgrade provides the HEP community with an unprecedented data sample taken at the frontier constituent energy which will be key to investigate the dynamic of EWSB and answer some of the most important open questions in particle physics.

The HL-LHC project is matched to a companion LHC detector upgrade program, to ensure that the detectors will keep their outstanding performance while operating with an average of ~140 underlying events. The 5×10^{34} cm^{-2}s^{-1} value for the luminosity leveling matches the nominal 25 ns bunch spacing: for a 50 ns bunch spacing the leveling value would be half value, only, with an inevitable loss of integrated luminosity. The experiments are actually designing the new upgraded detectors capable to *digest* a maximum of 200 events/crossing both for keeping a reasonable margin against shortfall (including a possible run of machine at 50 ns, would 25 ns become too difficult), and for taking into account the inevitable fluctuations around the average value. The LHC has provided collisions so far at 8 TeV center-of-mass energy, and with total beam currents of about 0.4 A (i.e. 70% of the nominal design value but with only half the nominal number of bunches). Once the magnet interconnections have been consolidated and the beam energy limits removed, as well as some radiation-to-electronic (R2E) intensity limits mitigated during LS1 in 2013-14, the design luminosity will hopefully be attained and eventually overcome in 2015. Once outstanding beam intensity limits in the injector chain and the LHC have been removed during additional shutdowns following the LS1, the LHC will head toward the so called *ultimate* design luminosity, which is about twice the nominal luminosity, i.e., 2×10^{34} cm^{-2}s^{-1}. This ultimate luminosity performance was planned to be reached by increasing the bunch population from 1.15 to 1.7×10^{11} protons, with a bunch spacing of 25 ns (beam current increases from 0.58 A to 0.86 A). Transforming this ultimate peak performance into a doubling of

parameter	LHC	HL-LHC	HE-LHC	VHE-LHC
c.m. energy [TeV]	14	14	33	100
circumference C [km]	26.7	26.7	26.7	80
dipole field [T]	8.33	8.33	20	20
dipole coil aperture [mm]	56	56	40	40
beam half aperture [cm]	2.2 (x), 1.8 (y)	2.2 (x), 1.8 (y)	1.3	1.3
injection energy [TeV]	0.45	0.45	>1.0	7.0
no. of bunches	2808	2808	1404	4210
bunch population [10^{11}]	1.125	2.2	1.62	1.34
init. transv. norm. emit. [μm]	3.73,	2.5	2.10	1.53
initial longitudinal emit. [eVs]	2.5	2.5	5.67	17.2
no. IPs contributing to tune shift	3	2	2	2
max. total beam-beam tune shift	0.01	0.015	0.01	0.01
beam circulating current [A]	0.584	1.12	0.412	0.338
rms bunch length [cm]	7.55	7.55	7.7	7.7
IP beta function [m]	0.55	0.15	0.3	1.5
init. rms IP spot size [μm]	16.7	7.1	6.0	6.5
full crossing angle [μrad]	285	590	240	52.3
stored beam energy [MJ]	362	694	601	4573
SR power per ring [kW]	3.6	6.9	82.5	1991
arc SR heat load dW/ds	0.21	0.40	3.5	84
energy loss per turn [keV]	6.7	6.7	201.3	5857
critical photon energy [eV]	44	44	575	5474
photon flux [10^{17}/m/s]	1.0	1.9	1.6	1.3
longit. SR emit. damping time [h]	12.9	12.9	1.0	0.32
horiz. SR emit. damping time [h]	25.8	25.8	2.0	0.64
init. longit. IBS emit. rise time [h]	57	21.0	78	305
d init. transv. IBS emit. rise time [h]	103	15.4	41	72.2
peak events per crossing	19	140 (lev.)	190	193
peak luminosity [10^{34} cm^{-2}s^{-1}]	1.0	7.4	5.0	5.0
beam lifetime due to burn off [h]	45	11.6	6.3	15.5
optimum run time [h]	15.2	8.9	7.0	11.8
opt. av. int. luminosity / day [fb^{-1}]	0.47	3.7	1.5	2.1

the annual integrated luminosity will however be very difficult and it is more likely that the result will be around 60-70 fb^{-1}/year.

4.2   Beam parameters

Experience with the LHC shows that the best set of parameters for actual operation is difficult to predict at this stage (before we obtain operational experience with the LHC at 7 TeV per beam). The upgrade studies should therefore provide the required HL-LHC performance over a wide range of parameters, and the machine and experiments will find eventually the best set of parameters in actual operations once the LHC probes the operation at maximum energy and with above nominal beam intensities.

The (instantaneous) luminosity L can be expressed as:

$$L = \gamma \frac{n_b N^2 f_{rev}}{4\pi \beta^* \epsilon_n} R; \quad R = \frac{1}{\sqrt{1 + \frac{\theta_c \sigma_z}{2\sigma}}} \tag{1}$$

where γ is the proton beam energy in unit of rest mass, n_b is the number of bunches in the machine: 1380 for 50 ns spacing and 2808 for 25 ns, N is the bunch population. $N_{nominal,25ns} = 1.15 \times 10^{11} p$ ($\implies$ 0.58A of beam current at 2808 bunches), f_{rev} is the revolution frequency (11.2 kHz), β^* is the beam beta function (focal length) at the collision point (nominal design 0.55 m), ϵ_n is the transverse normalized emittance (nominal design: 3.75 μm), R is a luminosity geometrical reduction factor (0.85 at 0.55 m of β^*, down to 0.5 at 0.25 m), θ_c is the full crossing angle between colliding beam (285 μrad as nominal design), σ, σ_z are the transverse and longitudinal r.m.s. size, respectively (16.7 μm and 7.55 cm). Table 4.2 lists the main parameters of the accelerators considered here. The parameters for the HL-LHC are given in the first column. The 25 ns bunch spacing is the nominal operating target. However a scheme with 50 ns is considered as fall-back solution. As previously mentioned, to reach the goal of 250 fb^{-1}/year with 160 days dedicated to proton physics, the efficiency must be 60%: a big leap forward is required on increasing availability (as previously mentioned) and turnaround time (time from end of physics to next start of physics). A margin that is not considered in the table is the possibility to work at β^* of 10 cm, which thanks to the ATS and larger Nb3Sn quadrupoles could be within reach.

The nominal total beam current of 1.11 A is a difficult target to attain. It represents hard limit for the LHC since it affects many systems, such as RF power systems and RF cavities, collimation, cryogenics, kicker magnets, vacuum system, beam diagnostics, in a direct way, and several others, like quench detection system of the SC magnets and virtually all controllers, in an indirect way, due to an increase of the R2E events. Transverse emittance is assumed to be very low also in view of the already better than the design value results during the first LHC running. However, getting the beam brightness, N_p/ϵ_n, required for HL-LHC is a very difficult challenge for the injector chain even after upgrades as well as for LHC to preserve it.

In view of these limitations, the classical route towards luminosity increase is the reduction of β^* by means of larger aperture triplet magnets for a given gradient or longer, larger aperture low-β triplet quadrupoles with a reduced gradient. However a reduction in β^* implies an increase of beam sizes over the whole matching section. Therefore the reduction in β^* implies not only larger triplet magnets but also larger separation/recombination dipoles and larger and/or modified matching section quadrupoles. A previous study showed that a practical limit in the LHC arises around β^* = 30-40 cm However, a novel scheme recently proposed (ATS) would allow to overcome these limitations in the LHC matching section. In this way a β^* value of 15 cm or even 10 cm can be envisaged and a flat optics with a β^* as low as 5 cm in the plane perpendicular to the crossing plane is possible. In particular, a value of β^*=10 cm has been recently attained in an LHC machine development run dedicated to test the ATS principle.
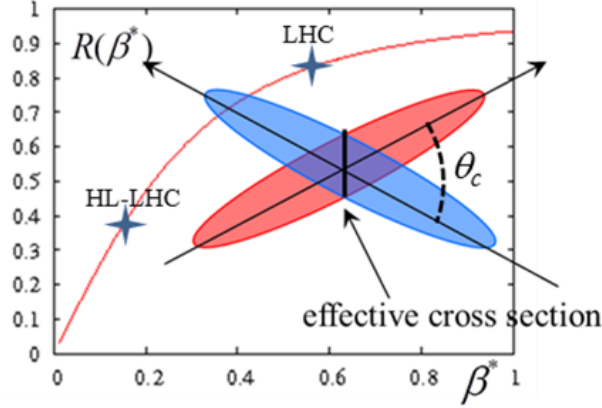
Figure 7: Geometrical reduction factor of luminosity vs. β^* with the two operating points for the nominal LHC and HL-LHC beam parameters indicated.

.

In order to be compatible with such small β^* values, we need to double the aperture of the low-β^* quadrupole magnets, which causes a peak field 50% higher that that of present LHC triplet magnets, requiring a new superconducting magnet technology based on Nb3Sn. The drawback of the very small β^* values is that they require a larger crossing angle, which entails in turn a reduction of the luminosity via the geometrical factor of beam overlap, R defined at Eq 1, compared to the LHC present conditions (see Figure 7). The reduction of the beam separation at the parasitic encounters and the mitigation of the beam-beam effects are under study but not yet proved. In the HL-LHC design, the reduction in the geometrical factor R is compensated with the use of crab cavities which rotate the beams before collisions to maximize their overlap. Their development is discussed in the next section.

5   Technology aspects

The present LHC is based on 30 years of development in the domain of superconducting (SC) magnet technologies. Nb-Ti based magnets are pushed to their limits: very compact two-in-one magnets provide 8.3 T operating field by using superfluid helium cooling.

The HL-LHC upgrade program requires quadrupoles with peak field in excess of 12 T, and heavily relies on the success of the advanced Nb3Sn technology developed by LARP, since the Nb-Ti superconductor used in the present LHC magnets cannot go beyond 9 T of field strength. Besides magnets, many other technologies are involved, like crab cavities, advanced collimators, SC links, advanced remote handling etc. The HL-LHC is a medium size project and implying deep changes over about 1.2 km of the LHC ring. Beside its physics goals, the HL-LHC will pave the way to a larger project like a higher energy LHC, which is based on a further enhancement of the same technologies. In fact, the technological development of high field magnets and other components discussed below, which are key to the HL-LHC program, connect the mid-term upgrade path of the LHC to the long-term developments
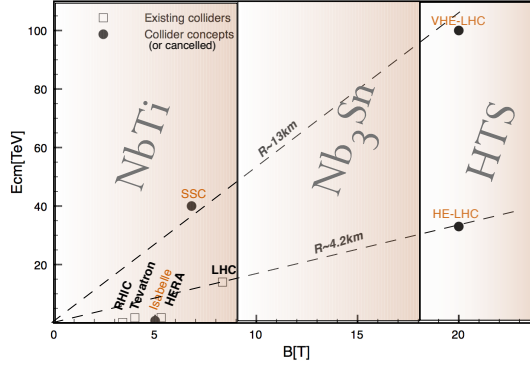
13

Figure 8: Role of the superconductor in the energy reach of hadron colliders as a function of field and radius.

towards hadron colliders of even higher energy. These programs have provided the US with unique know-hows at the national labs and recognized leadership in magnet R&D. They also have important overlaps with other HEP research areas such as the muon accelerator program (MAP) and accelerators for the intensity frontier, in the fields of magnet and collimation systems. The muon collider design requires dipoles of large field strength (10-20 T) and aperture (25 mm), high field solenoids and final focus quadrupoles. In addition to field strength, magnet programs need to take into consideration cost-effectiveness and scalability in magnet designs. The SC dipoles for a future collider will dominate the facility cost. Technically they are one of the highest-risk elements. Designs must be industrializable to leverage the strength of the private sector in providing cost-effective fabrication.

It is important to continue a focused integrated program emphasizing engineering readiness of technologies suitable for high energy hadron colliders with applications to the muon accelerator program and the intensity frontier.

In this section, we discuss the technological aspects of high field magnets from the conductor development to specific designs, the HL-LHC collimation issues and the crab cavity R&D.

5.1   Conductor development for SC magnets

Superconductor properties form the basis of magnet performance. The main low-temperature superconductors (LTS) used in accelerator magnets are NbTi and Nb_3Sn. All SC magnets for colliders to-date have been based on the LTS material NbTi, which has a critical field $B_{c2} \approx 11T$ at 1.8K. NbTi accelerator technology has been pushed to its limit in the LHC dipoles, with operating fields of 8.4T at 1.8K. Accelerator magnet research since then has therefore focused for the most part on the low-temperature superconductor Nb_3Sn, which has a critical field of $B_{c2} \approx 27T$ at 1.8K 9 and which can therefore provide access to fields beyond the intrinsic limitation of NbTi technology [?]. Nb_3Sn is a brittle inter-metallic compound, which imposes significant constraints on the design, fabrication and implementation of the
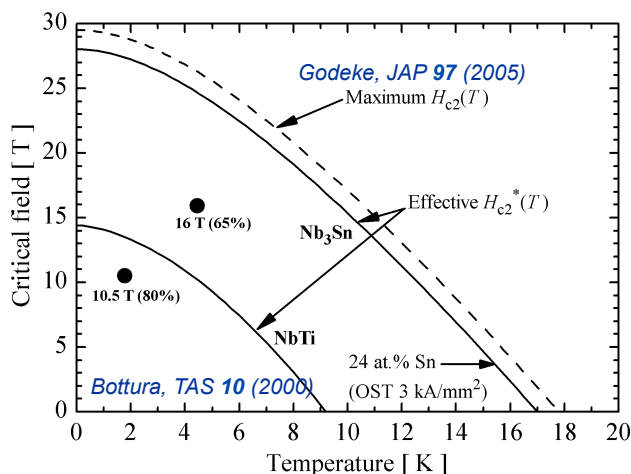
14

Figure 9: Plot of $J_c(B, 4.2K)$ for NbTi and Nb$_3$Sn.

material in accelerator magnets.

For Nb$_3$Sn, improvements in the current density, filament size, stability and production length properties has been the focus of the GARD-funded Conductor Development Program (CDP), initiated in 1999. CDP provides funds for the support of industrial improvements that are focused on specific target areas. Over the last ~ 15 years, the industry has made tremendous progress in Nb$_3$Sn: the current-density figure of merit $J_c(12T, 4.2K)$ has tripled to $J_c(12T, 4.2K) > 3000$A/mm^2. Ongoing efforts focus on reducing the D_{eff} by increasing the number of filaments in the wire, and in improving RRR through improvements in the barrier surrounding the filaments.

A fairly new area of conductor development pertains to high-temperature superconductors (HTS). The materials, primarily Bi$_2$Sr$_2$CaCu$_2$O$_x$ (Bi–2212) and YBa$_2$Cu$_3$O$_{7-\delta}$(YBCO), are under investigation for a high-field magnet applications: at low-temperatures (e.g. 1.8-4.5K) these materials exhibit good current densities at high magnetic fields; in fact $J_c(B)$ is nearly independent of field above ~ 10T. Over the last few years a collaboration of US national laboratories and university groups has worked to develop Bi-2212 as a viable conductor for magnet applications. Funded by the DOE OHEP and first formed as the "Very High Field Superconducting Magnet Consortium" (VHFSMC), the group worked with industry to develop a baseline round wire, demonstrated that the wire could by cabled into the standard Rutherford cable configuration for a current-scalable conductor, and designed, fabricated, and tested first solenoid and racetrack coils. The effort demonstrated basic viability of the conductor. However, it was clear that the effective ("engineering") current density (J_E) of the wire was not suitable for accelerator magnet application. A smaller, conductor-focused group, the "Bi-2212 Strand and Cable Collaboration" (BSCCo), was therefore formed to focus on J_E of Bi-2212. This effort was successful in demonstrating that, by modifying the processing to include high-pressure during the heat treatment, thereby dramatically reducing porosity in the final conductor, the J_E could be tripled. This development is now the focus of renewed interest by the magnet community, with active programs in place to demonstrate dipole and solenoid inserts for accelerator applications.
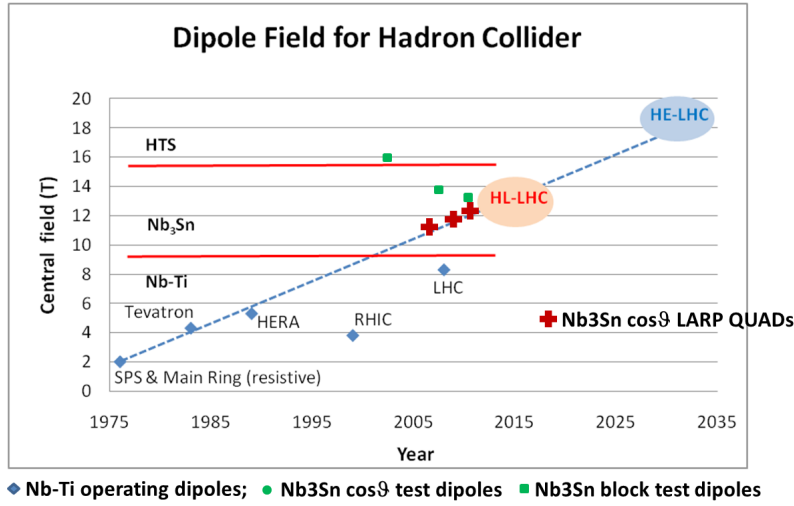
15

Figure 10:

Progress of accelerator magnets for hadron colliders: below 9 T it is the realm of Nb-Ti: here are reported nominal operating condition of Nb-Ti magnets used in the present machines; beyond 9 Tesla, Nb3Sn is needed: the results refers to prototype magnets and record field is reported rather than operating one. Early Nb3Sn dipoles have 50 mm bore while the HD series features an aperture of 40 mm. LARP magnets are quadrupoles, with 90 (LQ) or 120 (HQ) mm aperture. HL-LHC requires a 150 mm quadrupole aperture.

5.2 High field magnets for HL-LHC

The plot in Fig. 10 illustrates the progress over the years from the resistive magnet era and the jump in performance required by HL-LHC. The graph resumes also the result for the high energy machine, that will be discussed later.

Radiation escaping has two main effects: i) heat deposition that may limit the performance of the SC magnets by increasing the conductor temperature; ii) radiation damage, especially to insulation but also to metallic components. Radiation damage for magnets exposed to the radiation near the experiments is directly proportional to the integrated luminosity and might occur around an integrated luminosity of 300 fb^{-1}, which is probably a conservative estimate. Heat deposition may limit the peak luminosity at about 1.7 to $2.5 \times 10^{34} \mathrm{cm}^{-2}\mathrm{s}^{-1}$. In both cases this means that sometimes after 2020 we need to change the low-β quadrupole triplet. This is a unique chance to replace it with magnets of new generation, capable of higher performance and making the full system more robust against radiation and other factors which would otherwise reduce the availability of the machine. In addition to the replacement of the quadrupole, the whole Interaction Region (IR) zone needs to be redesigned with larger aperture D1/D2 (the pair of recombination/separation dipole magnets), with a new DFBX, the cryo-distribution electrical feed-box of the low-β triplet and with much better access to various equipment for maintenance, with an improvement of the cryogenic system and with the removal out of the tunnel of the most critical (as far
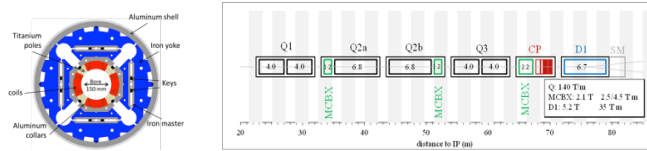
16

Figure 11: Left: cross section of the 150 mm aperture quadrupole of the inner triplet, under development by CERN and the US LARP program. Right: layout of the HL-LHC IR (inner triplet, correctors and D1).

as radiation exposure is concerned) power supplies and DFB associated. Power supplies and DFB would be relocated on ground surface, which will reduce the time of intervention and easy maintenance, by means of powerful 150 kA SC links. Many other systems (SC magnet protection, interlock, etc.) would also be upgraded to improve machine availability.

For accelerators we need a current density between of $J_c \simeq$ 2500-3000 A/mm^2 , about 3 times that used in the ITER magnets: this has been possible thanks to the long-term Conductor Development Program funded by DOE. Once the conductor becomes available, the magnet field progresses steadily as shown by the progress of the maximum field in short Nb3Sn dipole or quadrupole magnets (what we call models, typically 1 m long or less). Despite that for Nb3Sn record fields are reported, obtained after many quenches and in conditions far from operation, the HL-LHC region is within reach. Clearly the above graph shows the results of the effort of LARP and of the Magnet Basic Programs of the USA labs in Nb3Sn technology. One has to note that the LARP quadrupoles have reached the 12 T field level with aperture of 90-120 mm, much larger than the present LHC quadrupoles (56-70 mm) and already very near to the 150 mm aperture which sit h target for the HL-LHC: LARP is really instrumental for the success of the upgrade. In Fig. 5 the new triplet scheme for the upgrade is reported. The US contribution may consist in the production of half of the new quadrupoles (Q1 and Q3 for the four sides of the two interaction points). Special tungsten shielding will be placed inside inner bore to limit the radiation deposition to the same level of the nominal LHC, about 30 MGy, despite the ten time higher integrated luminosity.

5.3 High field magnet R&D for very high energy colliders

To clarify the driving issues in high-field dipole development, it is helpful to understand fundamental design limitations. The concept of a $Cos(\theta)$ dipole is shown in Fig. 12. Fig. 13 illustrates the fact that the field produced by a perfect $Cos(\theta)$ current density distribution is a function of the current density J_E and coil width w, and independent of the radius r. Hence the volume of conductor (V) needed to produce a field B_0 scales like $V \propto r$. This scaling can be improved by "grading" the conductor, i.e. leveraging the $J_c(B)$ behavior of superconductors to tailor the current density of the wire as a function of radial position, resulting in less conductor volume for a given field; the value of grading with Nb$_3$Sn is shown in Fig. 14. From Fig. 12 it is evident that the Lorentz force $F_\theta \sim J_E B_r$ accumulates along the azimuth, resulting in maximum stress $\sigma_{\theta m}$ on the midplane. Experience with Nb$_3$Sn magnets
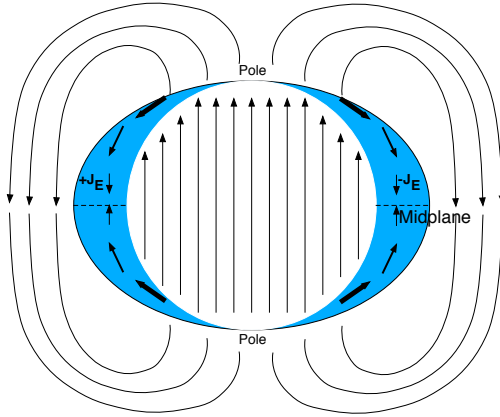
17

Figure 12: Schematic of a $Cos(\theta)$ current density distribution and azimuthal forces. Note that the forces accumulate on the azimuth, resulting in peak stress on the mid plane of a $Cos(\theta)$ dipole.
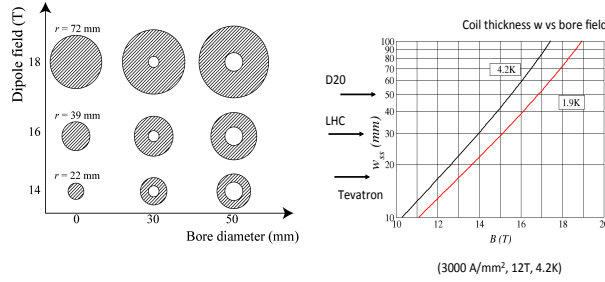

Figure 13: The field produced by a $Cos(\theta)$ current density distribution is a function of coil width and current density, but not of the coil radius.

has lead to well-established limitations $\sigma_{\theta m} < 200$MPa on the compressive mid plane stress; beyond this value the conductor degrades and magnet performance is unreliable. Due to the accumulation, stress on a $Cos(\theta)$ coil of radius r and thickness w scales as

$$\sigma_{\theta m} \propto r J_E / w; \tag{2}$$

implementing grading in a high field $Cos(\theta)$ dipole therefore results in dramatic increase in $\sigma_{\theta m}$, since w decreases and J_E increases with r when grading is incorporated. Fig. 14 provides an example for a Nb$_3$Sn $\sim$ 18T coil layout; note that the graded scenario far exceeds the stress limitation for the material.

Stress is therefore a dominant limitation to high-field dipole designs. From Eq. 2 it is evident that $\sigma_{\theta m}$ can be reduced to acceptable values by reducing the current density and making the coil cross-section larger; this comes at the expense of significant more conductor. Furthermore, the actual stress state in the $Cos(\theta)$ design is more complicated than described, with significant radial forces acting on the coils, again predominantly in the midplane region.

The importance of stress accumulation in dipole magnets has been recognized for some time. Alternative magnet designs, using "block" coils in various configurations, has been the focus of much effort over the last $\sim$ 15 years. A concept of stress management was proposed
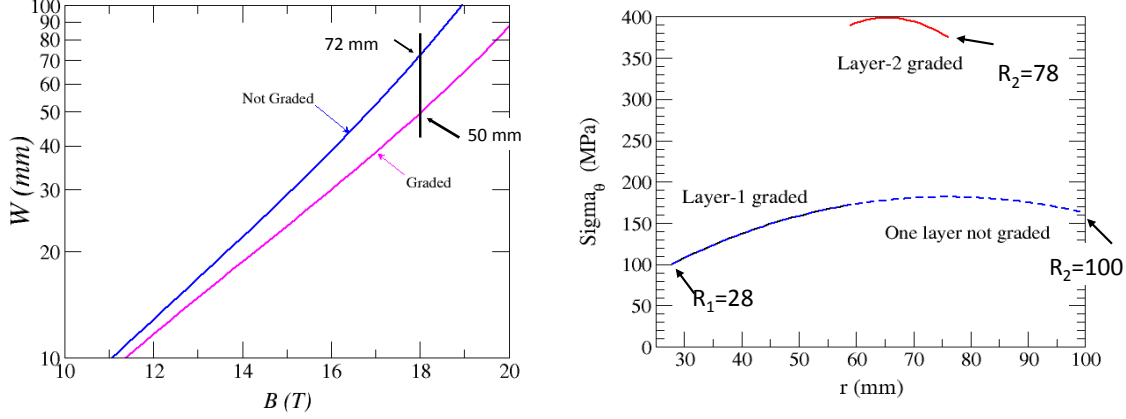
18

Figure 14: (Left) Improvement in field-generating efficiency of $Cos(\theta)$ current density distribution using "grading". (Right) Enhancement of $\sigma_{\theta m}$ associated with grading of a $Cos(\theta)$ magnet. Values correspond to a ~ 18T Nb_3Sn scenario.
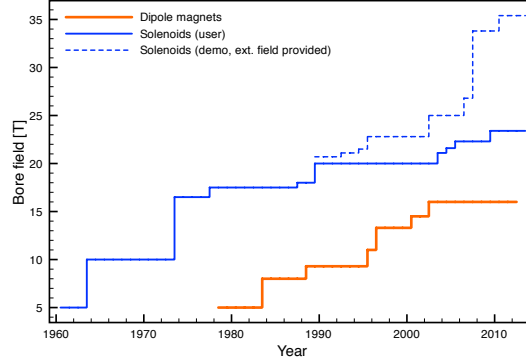

Figure 15: Progress in SC dipole magnet performance vs solenoids over the last few decades. Note the step increases, typically associated with significant material developments and/or new design paradigms. The dotted line represents prototype solenoids, where SC solenoids are tested in a background field provided by resistive magnets.

by the Texas A&M group [?]; the idea is to intercept stress before it can accumulate to unacceptable values. An alternative approach, using a "canted $Cos(\theta)$" design concept, is under investigation at LBNL [?, ?].

5.3.1 Magnet protection

Another important limitation of high-field dipoles and quadrupoles concerns the stored magnetic energy E_m. The use of high current density superconductors in magnets with stored energies $E_m \propto \pi r^2 B_0 L$, where L is the magnet length, results in significant heating of the magnet in the case of a quench (sudden irreversible loss of superconductivity at some point in the conductor). Highly specialized magnet protection circuitry is now employed in high-field accelerator magnets, typically incorporating the following features:
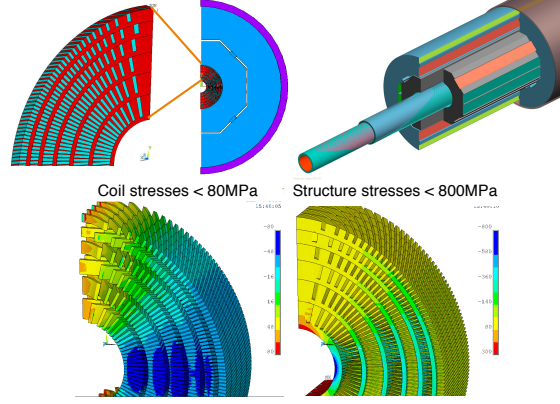
19

Figure 16: Concept of a Canted $Cos(\theta)$ magnet yielding 18T. The design, composed of 6 layers, uses graded Nb$_3$Sn Rutherford cable. Azimuthal forces acting on each cable are captured by the ribs; radial forces are supported via prestress from the external structure. Peak stresses on the conductor are significantly lower than on existing high-field dipoles, and an order of magnitude reduced from an equivalent $Cos(\theta)$ design.
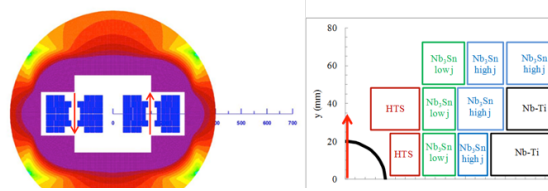

Figure 17: Concept of a Hybrid block-dipole magnet yielding 20T, courtesy E. Todesco, CERN. The design uses YBCO coils in the high-field region, Nb$_3$Sn in the "middle" field region, and NbTi in the low-field region. The design meets basic field quality requirements, but has not been fully evaluated in terms of mechanical stresses.

- fast detection of a quench onsite, typically within a few milliseconds of quench initiation - the detection must discriminate between real quench signals and false triggers emanating from flux jumps that can randomly occur;

- firing of heaters distributed in the magnet to force a large fraction of the superconductor into the normal (non-superconducting) state;

- activation of an external dump resistor to extract a significant fraction of the power away from the magnet.

All of these event must happen on a timescale of 10's of milliseconds in order to keep localized areas of the magnet from overheating. As current densities in superconductors improve, and higher-field and larger-bore magnets are developed, magnet protection becomes a significant technical challenge.

5.3.2   Field quality

Dipole magnets for a future collider will have strict requirements on multipole content and hysteresis. These issues are impacted by the choice/characteristics of superconductor and by the magnet design. SC wires are composed of a large number of filaments that are then twisted to minimize coupling losses, i.e. resistive Joule heating generated by dB/dt during magnet ramping. The filaments themselves can support persistent currents that impact field quality and are hysteric in nature. Furthermore, the filaments can experience sudden flux-penetration ("flux-jumps") as fields vary and the shielding nature of the superconductor is overwhelmed by the local Lorentz force acting on the pinned vortices. Although in most cases the superconductor can recover from such events, the resulting flux dynamics cause small field fluctuations that must be minimized.

These issues are addressed by minimizing the effective diameter of the filaments; this is an area of active development by industry, with support from the GARD CDP in the US. We note that the HTS materials Bi-2212 and YBCO both currently suffer from large effective filament sizes; significant advances will need to occur in the material technology for the conductors to be viable candidates for accelerator dipoles. Other magnet systems, such as interaction region (IR) quadrupoles and solenoids for a Muon collider, are much less sensitive to field quality concerns and may be early adopters of HTS materials in accelerators. The use of high T_c conductors gives an important temperature margin to these systems and needs to be a priority in the US HEP R&D program.

In terms of magnet design, field quality is dictated by the conductor layout in the coil cross section, a fairly well understood area. Issues include:

- Thorough understanding of fabrication and assembly tolerances and their impact on field quality;

- Understanding of the influence of thermal contraction and deflections associated with magnet energization, and their impact on field quality.
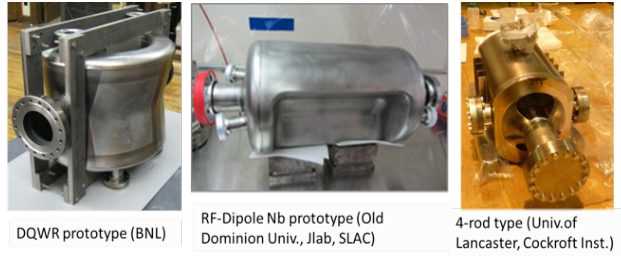
21

DQWR prototype (BNL) RF-Dipole Nb prototype (Old Dominion Univ., Jlab, SLAC) 4-rod type (Univ.of Lancaster, Cockroft Inst.)

Figure 18: The three types of compact crab cavity that are being pursued so far for HL-LHC.

5.4 Collimation

The LHC collimation system is operating well, but in order to cope with the higher beam energy density as well as to lower impedance will need to be renovated. Gains in triplet aperture and performance must be matched by an adequate consolidation or modification of the collimation system. In addition, a collimation system in the dispersion suppressor (DS) needs to be added to avoid the leakage of off-momentum particle, into the first and second main SC dipoles. This has been already identified as a possible LHC performance limitation. The most promising proposed concept requires to substitute one of the LHC main dipoles with a dipole of equal bending strength (121 T-m) of shorter length (11 m) and higher field (11 T) than those of the present LHC dipoles (8.3 T and 14.2 m). The gain in space is sufficient for placing special collimators to intercept the off-momentum particles. This new 11 T dipole, which is jointly developed by CERN and Fermilab will be actually realized with two cold masses of 5.5 m length, and should become the first magnet breaking through the 10 T frontier to be installed in a particle accelerator

5.5 Crab cavities

In order to preserve the luminosity at large crossing angle, crab cavities are adopted in the HL-LHC design. These crab cavities are not particularly demanding in terms of the required voltage. However, they go beyond the state-of-the art because the transverse cavity dimension is limited by the 194 mm distance between the two LHC beams, a value smaller than the $\lambda/4$ value of the 400 MHz wave, practically excluding the well-known elliptical cavity geometry. This request of small beam separation requires an unconventional, very compact design. Looking for an unconventional design approach different options were proposed and considered. After detailed studies and R&D three realistic design options have emerged as shown in Figure fig:crabs.

The first full test of a cavity prototype has just been completed for the RF-dipole type. It was operated well above the target value of 3.4 MV transverse voltage VT (see Figure 19), quenching at 7 MV and showing operational gradient at 5 MV. This result is very encouraging, though many other questions remain open, such as the cavity integration in a very compact cryostat. Critical issues about the use of crab cavities include their effect on the proton beam in term of noise-induced beam emittance growth and the understanding the
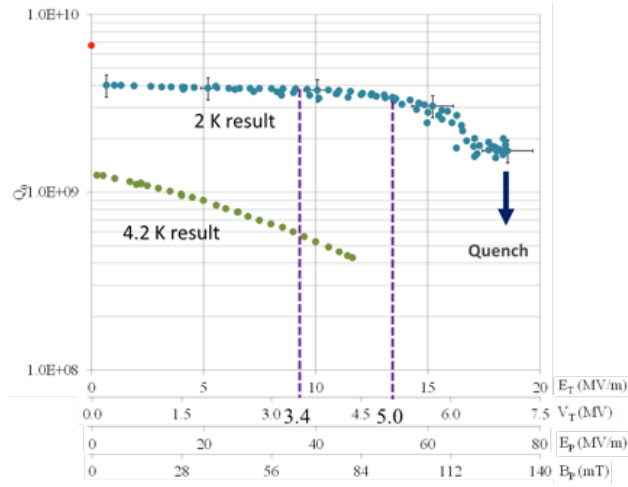
Figure 19: Results of the first full test of a crab cavity: the RF dipole (ODU-SLAC, LARP). Vertical lines represent indicate target voltage (3.4 MV) and actual usable voltage (5 MV). Beside transverse gradient and voltage, on the horizontal axis, the peak electric filed and magnetic field are reported, too. The test has been carried out at JLab.

possible failure modes, which must be carefully studied in order to allow safe operation of the machine.

Would the crab cavity not be usable for HL-LHC, the loss in luminosity can be minimized by colliding flat beams at the smallest possible crossing angle, by pushing the compensation for the LRbb interactions by electric wires.

6 Higher energy colliders

Given the progress in magnet technology and the maturity that Nb3Sn is reaching, thanks to the LARP program for HL-LHC, it is legitimate to forecast that Nb3Tn magnets with operating field (i.e with 15-20% margin w.r.t. quench) can reach its limit of 15.5-16 T in operative condition within the next decade, opening the path towards a collider with energy significantly larger compared to those of the LHC. This opens up the way towards very high energy hadron collisions which bring an exceptional potential for probing the energy frontier.

6.1 HE-LHC

The first option being considered is a machine housed in the LHC tunnel. The reachable center-of-mass energy depends on the dipole field strength. An energy of 26 TeV is within reach using Nb3Sn technology magnet, which makes a big advantage in reducing complexity and cost of the magnet system. This becomes ∼33 TeV if 20 T magnets are available, which would require magnets based on more futuristic HTS conductors. In this case the limited space available in the LHC tunnel represents an important problem to overcome. The inter-

beam distance must be increased to 300 mm in order to allow for thicker superconducting coils in the main dipoles and quadrupoles in order to generate the 20 T field. A 2D design of the magnet featuring an aperture of 40 mm and an operative field of 20 T with realistic superconductor current density in all coils block ($J = 400$ A/mm^2) has been initiated. Anticoils are needed to reduce stray field, collider field quality is not yet proved and magnet protection will be certainly an issue. A vigorous R&D program is needed to demonstrate the viability of HTS-based cables and the subsequent magnet engineering design. The inner block of HTS bring about 4-5 T, and they are necessary for the 20 T target.

The beam parameters for the HE-LHC are not too different compared to those for the LHC or HL-LHC. In this respect the machine design looks feasible. However, there are two areas which have been identified as critical, in addition to the magnets. First, the injection scheme relies on kickers more powerful than those used in LHC, which are already at the limit of current technology. Also the extraction system is critical, though to a lesser extent. An important program of R&D in fast pulsed- high-strength kickers is a necessary complement of the dipole magnet program. Then, the beam pipe and beam screen have to absorb a synchrotron radiation which is more than 20 times higher compared to the LHC. Synchrotron radiation is very beneficial for beam stabilization and will make the HE-LHC to be the first hadron machine dominated by synchrotron radiation dumping. However, the power dissipated in SR must be removed at cryogenic temperature. In LHC it is removed at 5-10 K. For the HE-LHC, a solution based on a beam screen at 40-60 K has been envisaged and has no major drawback, although careful design, engineering and prototyping need to be developed to prove this solution. The beam stability due to the increased wall resistance of beam screen seems to be within safe limits. A solution similar to that adopted at the LHC with a beam screen at 10 K will be heavy for the cryogenics. The additional 12 kW of power needed for each of the eight sectors would require to almost double the present 8×18 kW plants. In addition, the beam screen refrigeration will be complicated by need to increase the local heat removal by a factor of twenty, by means of higher pressure drop and increased cooling pipe conductance. This solution is certainly not impossible but better options seem viable. SR heat removal at higher temperature is the first. Vacuum stability indicates two possible windows for beam screen operation: 40-60 K (inlet-outlet temperature) and 85-100 K. The first option maintains the cryogenic power at 4.2 K equal to that of the LHC, the second makes a gain in refrigeration. However, the first option is preferable because the heat leakage from a higher temperature beam screen and the 1.8 K cold mass will be more than double in the second option and the electrical resistivity increases by a factor of 5 above the LHC value for the first option and a factor of 22 for the higher temperature option. The consequences of the higher resistivity on beam stability are not dramatic, because both transverse and longitudinal beam impedance increase with square root of the wall resistivity. The resistivity of copper at 50 K and 20 T is just a factor 2.5 more than the resistivity at 20 K, 8.3 T, making the impedance increasing of just 60%, a manageable factor. A thicker copper coating (in LHC is 75 μm) will partially compensate the increased resistivity, a compensation that is necessary to cut down image currents power losses, too. Despite that copper coating appears to be a viable solution for HE-LHC, use of YBCO coating ($T_c =$

85 K) on beam screen inner side can virtually null the resistance and solve out the problem: it will make possible even working at 100 K (if the thermal contact to the 1.9 K cold mass can be made very loose). This HTS coating is certainly more expensive and complex that the copper co-lamination of the LHC beam screen. However, given its potential, it should be carefully investigated as part of this R&D.

6.2 Proton Colliders beyond LHC

Studies for a very large proton collider able to deliver center-of-mass energies of order of 100 TeV (or more) have been already conducted from 1997 and subsequently updated, led by Fermilab (Design Study for a Staged VLHC, Report Fermilab TM-2149 (2001)). An update based on higher field magnets has been prepared and submitted as a white paper to this Community Summer Study. A study to investigate the feasibility of a 80-100 km ring for an next-generation hadron collider is now starting at CERN (VHE-LHC). The construction of a new tunnel relieves the pressure from the achievable dipole field strength, since this can be traded for the tunnel circumference. The target collision energy is 100 TeV for 20 T dipoles in an 80 km tunnel. However, an 100 km tunnel would provide the same collision energy of 100 TeV with reduced field of 16 T, reachable with Nb3Sn technology which a much more mature and less expensive conductor than HTS. The CERN civil engineer team has studied a 5 m diameter tunnel, compared to the 3.8 m of the present LHC tunnel thus allowing for larger cryo-modules. Cost and magnet technology put aside, the main issue for this collider is the removal of a synchrotron radiation. In a 80 km, 100 TeV proton collider, the dumped SR power will jump from the 3.6 kW/ring of the LHC and 82 kW/ring of a HE-LHC to ∼2 MW/ring. Dealing with this 500 times increase of SR compared to the present LHC value will be a major issue. While the beam stabilization will get a tremendous benefit, making the machine much easier from the point of view of the beam dynamics, we do not know if a beam screen cooled at 100 K (to limit thermodynamic load) would be capable to withstand the resulting heat deposition. In addition, the critical energy of the emitted photon is in the soft X-ray range and its effect on e-cloud and surface needs to be studied. The issue of synchrotron radiation removal is key to the machine feasibility. Photon stoppers, already envisaged for the US VLHC design, might be made to work but this has not yet been demonstrated. The first option would be to operate the beam screen in the temperature window of 85-100 K, good for vacuum stability. However, taking a COP (efficiency between cryo power and plug power) of 10, the 2×2 MW power removed at 90 K become approximately 2×20 MW in the cryogenic plant. Since the cryogenic power required by the whole ring is of the order of 120 MW (for 1.9 K magnets) or 40 MW (for 4.2 K magnets), the additional power consumption of 40 MW for removal of synchrotron radiation remains acceptable. However, the problem of keeping well insulated the beam screen (at 100 K) from the vacuum pipe (at 1.9 or 4.2 K) while removing longitudinally the 37 W/m inside the vacuum pipe represents a major challenge. The cooling pipe of the beam screen may become too large and require an increased magnet aperture, beyond the 40 mm, that has been the guideline for the HE and VHE-LHC magnets, so far. Another possible solution

is to investigate the possibility of letting the radiation escaping form the beam pipe and intercept it with a cold finger at a temperature to be optimized between 80 K and room temperature, as proposed in the US VLHC study. In the case the cold finger is kept at 80 K, the cryogenic load of 40 MW will remain, however the issue of local removal of the heat along the beam screen is avoided. The magnet aperture might need to be increased. A detailed study and optimization, which includes the length of the main dipoles, should establish the best solution. Although the problem of synchrotron radiation is challenging, it should not been considered to be a showstopper. The benefit of the strong damping due the synchrotron radiation at 50 TeV/beam should be underlined. Transverse damping time becomes about 30 minutes, to be compared to one day at the LHC, and this will greatly contribute to solve the issue of beam stability due to impedance or other collective effects. This would be a first time for an hadron collider. The coating of the beam screen with HTS, as proposed for a HE-LHC, may be not required for a long tunnel. The cryogenic system will be much more powerful than that installed at the LHC, because of the tunnel length and of SR power. It will represent a cost driver and will seriously impact the facility power consumption. A very preliminary estimate of the electrical power needed for the cryo-system is in the range of 150-200 MW.

It is important to ensure a significant US participation in the study of a high energy proton collider in a large tunnel. The study will capitalize on experience in the US community, will inform directions for an expanded US technology reach and guide the long term roadmap with strong synergies with the muon and intensity machines.

Conclusions

Acknowledgements

References

[1] Higgs Cross-Section WG, submission to the Cracow Symp. of the European Strategy Group,

  https://indico.cern.ch/contributionDisplay.py?contribId=176&confId=175067

[2] A. Donnachie and P. V. Landshoff, Phys. Lett. B **296** (1992) 227 [hep-ph/9209205].

[3] G. A. Schuler and T. Sjostrand, Phys. Rev. D **49** (1994) 2257.

[4] B. Abelev *et al.* [ALICE Collaboration], Eur. Phys. J. C **73** (2013) 2456 [arXiv:1208.4968 [hep-ex]].

[5] D. d'Enterria, R. Engel, T. Pierog, S. Ostapchenko and K. Werner, Astropart. Phys. **35** (2011) 98 [arXiv:1101.5596 [astro-ph.HE]].

[6] G. Aad *et al.* [ATLAS Collaboration], JHEP **1211** (2012) 033 [arXiv:1208.6256 [hep-ex]].

[7] A. Karneyeu, L. Mijovic, S. Prestel and P. Z. Skands, arXiv:1306.3436 [hep-ph].

[8] S. Chatrchyan *et al.* [CMS Collaboration], JHEP **1111** (2011) 148 [Erratum-ibid. **1202** (2012) 055] [arXiv:1110.0211 [hep-ex]].

[9] GAntchev *et al.* [TOTEM Collaboration], Europhys. Lett. **98** (2012) 31002 [arXiv:1205.4105 [hep-ex]].